References

BERTAUT, E. F., BLUM, P. & SAGNIÈRES, A. (1959). *Acta Cryst.* **12**, 149-159.
DOWNING, K. H., MEISHENG, H., WENK, H. R. & O'KEEFE, M. A. (1990). *Nature (London)*, **348**, 525-528.
ERCHARK, M., FANKUCHEN, J. I. & WARD, R. (1946). *J. Am. Chem. Soc.* **68**, 2085-2096.
GALLAGHER, P. K., MACCHESNEY, J. B. & BUCHANAN, D. N. E. (1965). *J. Chem. Phys.* **43**, 516-520.
GONZÁLEZ-CALBET, J. M., PARRAS, M., VALLET-REGÍ, M. & GRENIER, J. C. (1990). *J. Solid State Chem.* **86**, 149-159.
GRENIER, J. C., WATTIAUX, A., POUCHARD, M., HAGENMULLER, P., PARRAS, M., VALLET, M., GONZÁLEZ-CALBET, J. M. & ALARIO, M. (1989). *J. Solid State Chem.* **80**, 6-11.
HAUPTMAN, H. & KARLE, J. (1953). ACA Monograph No. 3. Ann Arbor: Edwards Brothers.
HOVMÖLLER, S. (1992). *Ultramicroscopy*, **41**, 121-135.
HOVMÖLLER, S., SJÖGREN, A., FARRANTS, G., SUNDBERG, M. & MARINDER, B.-O. (1984). *Nature (London)*, **311**, 238-241.
HOVMÖLLER, S., SJÖGREN, A. & WANG, D. N. (1988). *Prog. Biophys. Mol. Biol.* **51**, 131-163.
HOVMÖLLER, S., ZOU, X. D., WANG, D. N., GONZÁLEZ-CALBET, J. M. & VALLET-REGÍ, M. (1988). *J. Solid State Chem.* **77**, 316-321.
ICHIDA, T. (1973). *J. Solid State Chem.* **7**, 308-315.
LI, D. X. & HOVMÖLLER, S. (1988). *J. Solid State Chem.* **73**, 5-10.
LUCCINNI, E., MERIANI, S. & MINICHELLI, D. (1970). *Acta Cryst.* B**29**, 1217-1219.
MORI, S. (1965). *J. Am. Ceram. Soc.* **48**, 165.
NEGAS, T. & ROTH, R. (1969). *J. Res. Natl Bur. Stand. Sect. A*, **73**, 425-430.
PARRAS, M., FOURNES, L., GRENIER, J. C., POUCHARD, M., CALBET, J., VALLET, M. & HAGENMULLER, P. (1990). *J. Solid State Chem.* **88**, 261-268.
PARRAS, M., VALLET-REGÍ, M., GONZÁLEZ-CALBET, J. M., ALARIO, M. A., GRENIER, J. C. & HAGENMULLER, P. (1987). *Mater. Res. Bull.* **22**, 1413-1419.
RIETVELD, H. B. (1967). *Acta Cryst.* **22**, 151-152.
WANG, D. N., HOVMÖLLER, S., KIHLBORG, L. & SUNDBERG, M. (1988). *Ultramicroscopy*, **25**, 303-316.
ZANNE, M. (1973). PhD thesis, Univ. Nancy, France.
ZOU, X. D. & HOVMÖLLER, S. (1992). *Ultramicroscopy*. In the press.

Acta Cryst. (1993). A**49**, 35-45

Anisotropy of Anomalous Scattering in X-ray Diffraction. III. 'Forbidden' Axial Reflections in Space Groups up to Orthorhombic Symmetry

BY A. KIRFEL

Mineralogisches Institut, Universität Würzburg, Am Hubland, W-8700 Würzburg, Germany

AND W. MORGENROTH

Universität des Saarlandes, FR Kristallographie, W-6600 Saarbrücken 11, *Germany*

(*Received* 2 *September* 1991; *accepted* 18 *May* 1992)

Abstract

Kinematic single-crystal X-ray diffraction of totally polarized radiation is investigated for the presence of AAS (anisotropy of anomalous scattering). The developed model allows a clear distinction between geometric and structural aspects of the scattering. The former incorporates essentially an extension of the conventional polarization correction, the latter leads to a generalized structure factor. Both aspects are combined in the description of a structure-factor tensor that is defined in the diffractometer system and consists of a complex linear combination of six real basic tensors uniquely defining the dependence of a reflection intensity on both the scattering angle 2Θ and the azimuthal setting Ψ of the crystal. The complex coefficients of that structure-factor expansion are determined by the crystal structure, including the anisotropy of at least one atomic scattering factor. Under the limiting conditions of purely σ-polarized radiation and one 'edge atom' per asymmetric unit, effects of AAS on the systematically extinct ('forbidden') axial reflections in all monoclinic and orthorhombic space groups are studied. The compilation of the results offers both a concise survey over 23 unique cases of relevant symmetry and a practical guide to designing diffraction experiments. One possible application of FRED (forbidden reflection near-edge diffraction) is partial-structure determination, *i.e.* the location of an anisotropically resonant scattering 'edge atom' from the intensity variations $I(\mathbf{h}, \Psi)$. The method requires only AAS and a few reflections whose intensities are measured at selected azimuthal settings.

0108-7673/93/010035-11$06.00

1. Introduction

The availability of synchrotron sources permitting single-crystal X-ray diffraction studies with radiation of variable energy has prompted interest in anisotropic anomalous scattering (AAS) of atoms bonded in a crystal. AAS is a resonance effect that can occur in the vicinity of an absorption edge, *i.e.* in the XANES and EXAFS regions. It can be modelled by an atomic scattering factor including energy-dependent anisotropic anomalous-dispersion correction terms that are represented by symmetric second-rank tensors, $\mathbf{f}'$, $\mathbf{f}''$, that are compatible with the atom's site symmetry.

Based on earlier studies by Templeton & Templeton (1980, 1982, 1985, 1988) and Dmitrienko (1983, 1984), a general formalism describing kinematic scattering from a single crystal in the presence of AAS and experimental evidence for the validity of the model have been given in previous contributions [Kirfel & Petcov (1992); Kirfel, Petcov & Eichhorn (1991); hereafter referred to as KP*b* and KPE, respectively]. A similar study of the problem was reported by Fanchon & Hendrickson (1990).

In general, AAS affects all reflections. Thus, it may be considered an unwanted effect in near-edge data collection to be circumvented by careful choice of the wavelength. On the other hand, AAS possesses exciting and potentially useful features. One of them is the violation of systematic extinction rules due to screw axes and/or glide planes in a structure, referred to as FRED (forbidden-reflection near-edge diffraction, see KPE). The factors determining the intensities of such 'forbidden' reflections can be summarized in two groups:

(i) the scattering angle 2Θ;

(ii) the Ψ setting of the crystal, *i.e.* rotation around the scattering vector $\mathbf{h}$;

(iii) the energy and the polarization of the incident radiation;

and

(iv) the resonant scattering of the 'edge atom(s)', *i.e.* $\mathbf{f}'(E), \mathbf{f}''(E)$;

(v) the partial structure of the 'edge atom(s)';

(vi) the occupation of the atomic site under consideration.

The factors of the first group can be varied by the experimentalist, the second group comprises solely sample properties.

The selectivity of scattering (v) from the 'edge atoms' alone renders the signal independent of the size and complexity of the nonresonant scattering 'rest structure'. If one confines the partial structure to one unique 'edge atom' per asymmetric unit, partial-structure information can be extracted from the intensity variations $I(\mathbf{h}, \Psi)$ of 'forbidden' reflections as first shown by Templeton & Templeton (1986) for $NaBrO_3$, with space group $P2_13$. A second proof has been given by Kirfel & Petcov (1992, KP*b*), applying an earlier proposed method [Kirfel & Petcov (1991), hereafter referred to as KP*a*] to a crystal of $LiHSeO_3$ with space group $P2_12_12_1$.

In the present contribution, our considerations about partial-structure information are extended to all monoclinic and orthorhombic space groups permitting FRED. Common to these is the presence of 2_1 screw axes and/or glide planes of type *a*, *b*, *c*, *n* or *d*.

In § 2, the general scattering algorithm (KPE) incorporating AAS is re-evaluated from a somewhat different viewpoint. The structure-factor tensor $\mathbf{F}(\mathbf{h})_D$, defined with respect to the diffractometer system, is expanded into a linear combination of a set of basic tensors, which determine exclusively the geometric part (i, ii) of the scattering. The complex coefficients of this expansion depend only on items (iv)-(vi), where (v) incorporates the space-group symmetry. Thus, § 2 of this paper is as general as possible and applies to any crystal symmetry.

Using this approach, §§ 3 and 4 deal with the intensities of 'forbidden' reflections and with the partial-structure information that can be obtained from them under the following conditions.

(i) The incident radiation is purely σ polarized. This condition is approximated by using synchrotron radiation and scattering in the vertical plane. (Extension to more general polarization properties is possible, but not helpful for the aim of this study.)

(ii) There is only one atom of an 'edge element' in the asymmetric unit.

(iii) Only the 'forbidden' *axial* reflections are considered in monoclinic and orthorhombic space groups.

(iv) Anisotropy of absorption is neglected.

The complex coefficients of the structure-factor tensor expansion are first evaluated and summarized for all relevant space groups belonging to a given point group. Then, 'polarized structure factors' (PSF), *i.e.* complex numbers, determining the σ- and π-polarized contributions to the scattered radiation are developed. This leads to a survey of the properties of FRED. Finally, the results are discussed in terms of partial-structure information, showing that all space groups can be covered by only a few different cases and that 'edge-atom' positions can be assessed provided AAS occurs to a significant degree. (This is the *only* prerequisite; no further knowledge about the resonance effect is required.)

Thus, the aim of §§ 3 and 4 of this contribution is to give not only a systematic survey over the relations between space-group symmetry and FRED but also a practical guide for the design of a diffraction experiment in order to yield partial-structure information. Since all results are presented for an atom in a general position, predictions of special effects due to positions with higher point symmetry can be easily derived.

2. The general Bragg-scattering formalism

2.1. *The structure-factor tensor in the diffractometer system*

The introduction of symmetric complex scattering-factor tensors **f** for anisotropically resonant scattering atoms leads to the formulation of a structure factor

$$\mathbf{F(h)} = \sum_{l=1}^{n} \sum_{p=1}^{m} o_l \mathbf{f}_{lp} T_{lp} G_{lp}, \tag{1}$$

where n is the number of atoms in the asymmetric unit; m is the number of symmetry operations of the space group; o_l is the occupation factor for site l (multiplicity); $T_{lp} = \exp[-\mathbf{h}^T \mathbf{B}_{lp} \mathbf{h}]$, the temperature-factor expression; $G_{lp} = \exp[2\pi i \mathbf{h} \cdot \mathbf{r}_{lp}]$, the geometric factor. $\mathbf{f}_{lp}$ is the scattering-factor tensor of the lth atom transformed by the rotational part of the pth symmetry operation of the space group according to

$$\mathbf{f}_{lp} = \mathbf{R}_p \mathbf{f}_{l1} \mathbf{R}_p^T. \tag{2}$$

$\mathbf{f}_{l1}$ is, of course, energy dependent and the real and imaginary parts generally exhibit different dependencies.

Each $\mathbf{f}_{lp}$ can be expanded into a linear combination of symmetric tensors $\mathbf{Q}_{ij}$,

$$\mathbf{f}_{lp} = \sum_{\substack{i,j=1 \\ i \le j}}^{3} f_{ij,lp} \mathbf{Q}_{ij}, \tag{3}$$

where the complex coefficients $f_{ij,lp}$ incorporate the transformations $\mathbf{R}_p$. The $\mathbf{Q}_{ij}$ are given by

$$\mathbf{Q}_{11} = \begin{pmatrix} 1 & 0 & 0 \\ 0 & 0 & 0 \\ 0 & 0 & 0 \end{pmatrix}, \quad \mathbf{Q}_{22} = \begin{pmatrix} 0 & 0 & 0 \\ 0 & 1 & 0 \\ 0 & 0 & 0 \end{pmatrix},$$

$$\mathbf{Q}_{33} = \begin{pmatrix} 0 & 0 & 0 \\ 0 & 0 & 0 \\ 0 & 0 & 1 \end{pmatrix}, \quad \mathbf{Q}_{12} = \begin{pmatrix} 0 & 1 & 0 \\ 1 & 0 & 0 \\ 0 & 0 & 0 \end{pmatrix}, \tag{4}$$

$$\mathbf{Q}_{13} = \begin{pmatrix} 0 & 0 & 1 \\ 0 & 0 & 0 \\ 1 & 0 & 0 \end{pmatrix}, \quad \mathbf{Q}_{23} = \begin{pmatrix} 0 & 0 & 0 \\ 0 & 0 & 1 \\ 0 & 1 & 0 \end{pmatrix}.$$

Then, the structure factor becomes (for radiation of constant energy)

$$\mathbf{F(h)} = \sum_{\substack{i,j=1 \\ i \le j}}^{3} A_{ij} \mathbf{Q}_{ij},$$

$$A_{ij} = \sum_{l}^{n} \sum_{p}^{m} o_l f_{ij,lp} T_{lp} G_{lp}. \tag{5}$$

To obtain $\mathbf{F(h)}$ with respect to the diffractometer system D (Fig. 1) as convenient for the description of the scattering (KPE), $\mathbf{F(h)}$ of (5) must first be transformed into a Cartesian system C fixed with respect to the crystal. If one chooses $X_C \| \mathbf{a}_0^*$, Y_C in the plane of $\mathbf{a}_0^*$ and $\mathbf{b}_0^*$, Z_C along $\mathbf{c}_0$, this is accomplished by transformation with an upper triangular matrix

$$\mathbf{B}_0 = \begin{pmatrix} 1 & \cos\gamma^* & \cos\beta^* \\ 0 & \sin\gamma^* & -\sin\beta^* \cos\alpha \\ 0 & 0 & V_0^*/\sin\gamma^* \end{pmatrix}, \tag{6}$$

$$V_0^* = (1 - \cos^2\alpha^* - \cos^2\beta^* - \cos^2\gamma^* + 2\cos\alpha^* \cos\beta^* \cos\gamma^*)^{1/2}.$$

$\mathbf{B}_0$ describes the unit vectors of the reciprocal lattice with respect to system C; $\mathbf{B}_0 = \mathbf{I}$ for orthogonal axes. The definition of C is the keeping with the literature (Busing & Levy, 1967; Willis & Pryor, 1975),

$$\mathbf{F(h)}_C = (\mathbf{B}_0^{-1})^T \mathbf{F(h)} (\mathbf{B}_0^{-1}). \tag{7}$$

Then, the crystal must be rotated into the diffraction position, so that $\mathbf{F(h)}_D$ defined with respect to the diffractometer system is given by

$$\mathbf{F(h)}_D = (\mathbf{X}_0 \mathbf{\Phi}_0) \mathbf{F(h)}_C (\mathbf{X}_0 \mathbf{\Phi}_0)^T. \tag{8}$$

$\mathbf{X}_0$ and $\mathbf{\Phi}_0$ are rotation matrices of the type

$$\mathbf{X}_0 = \begin{pmatrix} \cos\xi & 0 & \sin\xi \\ 0 & 1 & 0 \\ -\sin\xi & 0 & \cos\xi \end{pmatrix},$$

$$\mathbf{\Phi}_0 = \begin{pmatrix} \cos\varphi & -\sin\varphi & 0 \\ \sin\varphi & \cos\varphi & 0 \\ 0 & 0 & 1 \end{pmatrix}. \tag{9}$$

Similar to (5), the resulting structure-factor tensor (8) can then be expressed as a linear combination,

$$\mathbf{F(h)}_D = \sum_{\substack{i,j=1 \\ i \le j}}^{3} A_{ij} (\mathbf{X}_0 \mathbf{\Phi}_0)(\mathbf{B}_0^{-1})^T \mathbf{Q}_{ij} (\mathbf{B}_0^{-1})(\mathbf{X}_0 \mathbf{\Phi}_0)^T$$

$$= \sum_{\substack{u,v=1 \\ u \le v}}^{3} F_{uv} \mathbf{Q}'_{uv}. \tag{10}$$

In this notation, the complex coefficients F_{uv} ($u, v = x, y, z$) are determined by the A_{ij} of (5) and by the elements of $\mathbf{B}_0$, $\mathbf{X}_0$ and $\mathbf{\Phi}_0$. Apart from the indices 1, 2, 3 being replaced by x, y, z, the $\mathbf{Q}'_{uv}$ take the same form as in (4), however, they are now defined in the Cartesian system D. The index surfaces of the $\mathbf{Q}'_{uv}$, *i.e.* $\mathbf{e}^T \mathbf{Q}'_{uv} \mathbf{e}$ ($\mathbf{e}$ is a unit vector) are recognized as surface spherical harmonics. The first three types correspond to squared dipoles p_x^2, p_y^2, p_z^2 oriented along the directions $[100]_D, [010]_D, [001]_D$ of system D, the latter three to quadrupoles d_{xy}, d_{xz}, d_{yz} with their positive lobes oriented along $[110]_D, [101]_D$ and $[011]_D$, respectively. Hence one can consider the index surface of any structure-factor tensor $\mathbf{F(h)}_D$ as a complex linear combination of six basic multipoles.

A rotation of the crystal around the scattering vector $\mathbf{h}$ ($\|X_D$) is described by

$$\mathbf{\Psi} = \begin{pmatrix} 1 & 0 & 0 \\ 0 & \cos\Psi & \sin\Psi \\ 0 & -\sin\Psi & \cos\Psi \end{pmatrix}. \tag{11}$$

(The setting of the crystal after rotation into the diffracting position is defined as $\Psi = 0$.) $\mathbf{\Psi}$ transforms the structure-factor tensor $\mathbf{F}(\mathbf{h})_D$ and the basic tensors according to

$$\begin{aligned} \mathbf{F}(\mathbf{h}, \Psi)_D &= \mathbf{\Psi}\mathbf{F}(\mathbf{h})_D\mathbf{\Psi}^T, \\ \mathbf{Q}'_{uv}(\Psi) &= \mathbf{\Psi}\mathbf{Q}'_{uv}\mathbf{\Psi}^T (u, v = x, y, z) \end{aligned} \tag{12}$$

and the Ψ dependence of the index surface of $\mathbf{F}(\mathbf{h}, \Psi)_D$ must be contained in the multipoles as viewed along $[100]_D$.

2.2. *The scattering contributions and basis functions*

The next stage of the analysis depends on equations (1)-(8) of KPE. A totally polarized electromagnetic plane wave is represented by an electric-field vector

$$\mathbf{E} = \begin{pmatrix} E_{0\sigma} \\ E_{0\pi} \end{pmatrix},$$

where the $E_{0\sigma,\pi}$ are generally complex numbers and σ and π denote the components perpendicular and parallel to the scattering plane (Fig. 1). The total intensity of the radiation scattered is then given by

$$I(\mathbf{h}, \Psi) = \langle \mathbf{E}^* | \mathcal{F}^+(\mathbf{h}, \Psi)\mathcal{F}(\mathbf{h}, \Psi) | \mathbf{E} \rangle. \tag{13}$$

The superscripts $^+$ and * denote the Hermitian and complex conjugates, respectively, and $\mathcal{F}(\mathbf{h}, \Psi)$ is a scattering matrix

$$\mathcal{F}(\mathbf{h}, \Psi) = \begin{pmatrix} \Phi_{\sigma'\sigma}(\mathbf{h}, \Psi) & \Phi_{\sigma'\pi}(\mathbf{h}, \Psi) \\ \Phi_{\pi'\sigma}(\mathbf{h}, \Psi) & \Phi_{\pi'\pi}(\mathbf{h}, \Psi) \end{pmatrix} \tag{14}$$

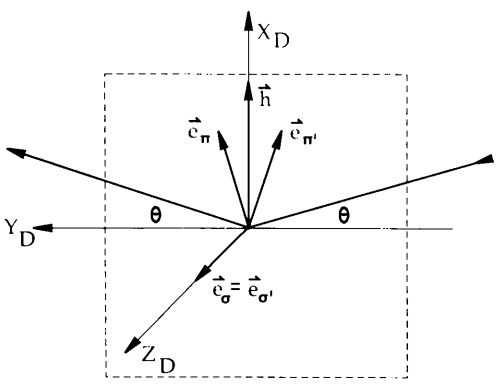

Fig. 1. Scattering geometry for the diffractometer system D in the reflection position. The vertical scattering plane contains $\mathbf{e}_\pi$ and $\mathbf{e}_{\pi'}$.

with

$$\begin{aligned} &\Phi_{\eta\nu}(\mathbf{h}, \Psi) = \mathbf{e}_\eta^T \mathbf{F}(\mathbf{h}, \Psi)_D \mathbf{e}_\nu \\ &(\eta = \sigma', \pi' \text{ and } \nu = \sigma, \pi). \end{aligned} \tag{15}$$

$\mathbf{e}_\sigma = \mathbf{e}_{\sigma'}$, $\mathbf{e}_\pi$ and $\mathbf{e}_{\pi'}$ are the unit vectors of the polarization directions defined in system D (Fig. 1). $\Phi_{\sigma'\pi}(\mathbf{h}, \Psi)$ describes the σ-polarized scattered radiation stemming from the π component of the primary radiation *etc.* The $\Phi_{\eta\nu}(\mathbf{h}, \Psi)$, being complex numbers, can be considered as 'structure factors including polarization effects', PSF, and are thus dependent on the type of scattering.

With reference to (10) and (12), each $\Phi_{\eta\nu}(\mathbf{h}, \Psi)$ can also be written as a linear combination, the $\mathbf{Q}'_{uv}$ of (10) being, however, replaced by

$$q_{uv}(\eta\nu, \Psi) = \mathbf{e}_\eta^T \mathbf{Q}'_{uv}(\Psi)\mathbf{e}_\nu. \tag{16}$$

The resulting real functions $q_{uv}(\eta\nu, \Psi)$ depend only on the azimuth, Ψ, and the scattering angle, 2Θ. They provide a set of simple trigonometric expressions each being characteristic for a particular combination of a $\mathbf{Q}'_{uv}$ with a type of scattering $\eta\nu$. Thus, the $q_{uv}(\eta\nu, \Psi)$ describe completely the geometric aspect of the scattering and any resulting intensity $I(\mathbf{h}, \Psi)$ is necessarily a function of them. It is therefore justified to consider the scattering in terms of scattering from the 'multipoles', *i.e.* to evaluate the basis functions $q_{uv}(\eta\nu, \Psi)$. The coefficients F_{uv} of (10) are then the weights applied to these functions. For a given reflection $\mathbf{h}$, azimuth Ψ and constant energy, these weights are solely determined by the physical aspect of the scattering, *i.e.* the space group, the positions, the occupation and the anisotropic scattering factors of the 'edge atoms'.

2.3. *The general geometric scattering terms*

From Fig. 1,

$$\begin{aligned} \mathbf{e}_\sigma = \mathbf{e}_{\sigma'} &= \begin{pmatrix} 0 \\ 0 \\ 1 \end{pmatrix}, \quad \mathbf{e}_\pi = \begin{pmatrix} \cos\Theta \\ \sin\Theta \\ 0 \end{pmatrix}, \\ \mathbf{e}_{\pi'} &= \begin{pmatrix} \cos\Theta \\ -\sin\Theta \\ 0 \end{pmatrix} \end{aligned} \tag{17}$$

and with the abbreviations

$$\begin{aligned} &C_\Psi = \cos\Psi, \quad S_\Psi = \sin\Psi, \quad C_{2\Psi} = \cos 2\Psi, \\ &S_{2\Psi} = \sin 2\Psi, \quad C_\Theta = \cos\Theta, \quad S_\Theta = \sin\Theta, \end{aligned} \tag{18}$$

one obtains the functions $q_{uv}(\eta\nu, \Psi)$, summarized in Table 1. Since the $q_{uv}(\sigma'\sigma, \Psi)$ are the values of their respective tensors $\mathbf{Q}'_{uv}$ in the direction of $\mathbf{e}_\sigma = [001]_D$, $\Phi_{\sigma'\sigma}(\mathbf{h}, \Psi)$ probes the index surface of $\mathbf{F}(\mathbf{h}, \Psi)_D$. Thus, $\Phi_{\sigma'\sigma}(\mathbf{h}, \Psi)$ is the value that the structure-factor tensor takes along the same direction as the crystal rotates around $\mathbf{h}\|[100]_D$. This function

Table 1. *Ψ and Θ dependencies of the basis functions $q_{uv}(\eta\nu, \Psi)$*

	$\sigma'\sigma$	$\pi'\pi$	$\pi'\sigma$	$\sigma'\pi$
q_{xx}	0	C_Θ^2	0	0
q_{yy}	S_Ψ^2	$-S_\Theta^2 C_\Psi^2$	$\frac{1}{2}S_\Theta S_{2\Psi}$	$-\frac{1}{2}S_\Theta S_{2\Psi}$
q_{zz}	C_Ψ^2	$-S_\Theta^2 S_\Psi^2$	$-\frac{1}{2}S_\Theta S_{2\Psi}$	$\frac{1}{2}S_\Theta S_{2\Psi}$
q_{xy}	0	0	$-C_\Theta S_\Psi$	$-C_\Theta S_\Psi$
q_{xz}	0	0	$C_\Theta C_\Psi$	$C_\Theta C_\Psi$
q_{yz}	$-S_{2\Psi}$	$-S_\Theta^2 S_{2\Psi}$	$-S_\Theta C_{2\Psi}$	$S_\Theta C_{2\Psi}$

is, of course, independent of the scattering angle. As expected, all other PSFs involving electric-field components in the scattering plane do depend on Θ. Table 1 shows in addition that the Ψ dependence of $I(\mathbf{h}, \Psi)$ - regardless of crystal system and space group - must be periodic in $2\pi/n$, where $n = 1, 2, 4$.

3. Intensities of 'forbidden' axial reflections in monoclinic and orthorhombic space groups

Under the limitations outlined in the *Introduction* and neglecting the temperature factor [see (1)] the structure-factor tensor in the presence of AAS is

$$\mathbf{F}(\mathbf{h}) = \sum_{p=1}^{m} o\mathbf{f}_p \exp[2\pi i \mathbf{h}\cdot\mathbf{t}_p] \exp[2\pi i \mathbf{h}\mathbf{R}_p\mathbf{r}], \quad (19)$$

where the symmetry-equivalent atom positions are given by

$$\mathbf{r}_p = \mathbf{t}_p + \mathbf{R}_p\mathbf{r}. \quad (20)$$

The elements t_{ip} of the translation vector $\mathbf{t}_p$ are either 0 or $\frac{1}{2}$ and the rotation matrices $\mathbf{R}_p$ possess only the diagonal elements $R_{ii,p} = \pm 1$ $(i = 1, 2, 3)$. For the two space groups *Fdd*2 and *Fddd*, t_{ip} can also take the values $\frac{1}{4}$ and $\frac{3}{4}$ and the 'forbidden' axial reflections are even. Then, for any 'forbidden' axial reflection, $2\mathbf{h}\cdot\mathbf{t}_p$ is either zero or an odd number, yielding

$$\exp[2\pi i \mathbf{h}\cdot\mathbf{t}_p] = (-1)^{2\mathbf{h}\cdot\mathbf{t}_p} = s_p. \quad (21)$$

The last factor of (19) is explicitly

$$\exp[2\pi i \mathbf{h}\mathbf{R}_p\mathbf{r}] = \cos[2\pi(hR_{11,p}x + kR_{22,p}y + lR_{33,p}z)] + i\sin[2\pi(hR_{11,p}x + kR_{22,p}y + lR_{33,p}z)]. \quad (22)$$

The scattering-factor tensor of symmetry-equivalent 'edge atoms', as given by (2), is

$$\mathbf{f}_p = \begin{pmatrix} f_{11} & R_{11,p}R_{22,p}f_{12} & R_{11,p}R_{33,p}f_{13} \\ R_{11,p}R_{22,p}f_{12} & f_{22} & R_{22,p}R_{33,p}f_{23} \\ R_{11,p}R_{33,p}f_{13} & R_{22,p}R_{33,p}f_{23} & f_{33} \end{pmatrix}. \quad (23)$$

With use of the fact that, for all p,

$$\cos[2\pi h R_{ii,p}x] = \cos[2\pi hx]$$
$$\sin[2\pi h R_{ii,p}x] = R_{ii,p}\sin[2\pi hx] \quad (24)$$

and with the abbreviations

$$C_{hx} = \cos[2\pi hx] \quad \text{and} \quad S_{hx} = \sin[2\pi hx]$$

etc. for C_{ky}, S_{ky}, C_{lz} and S_{lz}, one can rewrite the structure-factor expression as

$$\begin{aligned}\mathbf{F}(\mathbf{h}) = \sum_{p=1}^{m} os_p\mathbf{f}_p\{&[C_{hx}C_{ky}C_{lz} - R_{22,p}R_{33,p}C_{hx}S_{ky}S_{lz} \\ &- R_{11,p}R_{22,p}S_{hx}S_{ky}C_{lz} - R_{11,p}R_{33,p}S_{hx}C_{ky}S_{lz}] \\ &+ i[R_{11,p}S_{hx}C_{ky}C_{lz} + R_{22,p}C_{hx}S_{ky}C_{lz} \\ &+ R_{33,p}C_{hx}C_{ky}S_{lz} - \det(\mathbf{R}_p)S_{hx}S_{ky}S_{lz}]\} \\ = \sum_{p=1}^{m} os_p\mathbf{f}_p X(\mathbf{h})_p \\ = \sum_{\substack{i=1 \\ i<j}}^{3}\sum_{p=1}^{m} os_p X(\mathbf{h})_p R_{ii,p}R_{jj,p}f_{ij}\mathbf{Q}_{ij}. \end{aligned} \quad (25)$$

In this equation, there are only matrices $\mathbf{Q}_{ij}$ with $i<j$. The contributions $\mathbf{Q}_{ij}$ with $i=j$ vanish, because the extinction rules apply to the diagonal elements of (23). For the 'forbidden' axial reflections, the $X(\mathbf{h})_p$ reduce to

$$\begin{aligned} X(h00)_p &= C_{hx} + iR_{11,p}S_{hx}, \\ X(0k0)_p &= C_{ky} + iR_{22,p}S_{ky}, \\ X(00l)_p &= C_{lz} + iR_{33,p}S_{lz}. \end{aligned} \quad (26)$$

Calculating (25) explicitly, one obtains sums over integer combinations that are abbreviated as

$$\begin{aligned} \sum_{p=1}^{m} s_p R_{ii,p} &= \sum_i, \\ \sum_{p=1}^{m} s_p R_{ii,p}R_{jj,p} &= \sum_{ij}, \\ \sum_{p=1}^{m} s_p \det(\mathbf{R}_p) &= \sum_{123}, \end{aligned} \quad (27)$$

where s_p depends, of course, on $\mathbf{h}$. Incorporating the space-group symmetry, these $\sum$ sums enter the coefficients A_{ij} of (5). The $\mathbf{F}$ tensors of the 'forbidden' axial reflections can be recast in the abbreviated notation

$$\begin{pmatrix} \mathbf{F}(h00) \\ \mathbf{F}(0k0) \\ \mathbf{F}(00l) \end{pmatrix} = o\mathbf{D}\begin{pmatrix} f_{12}\mathbf{Q}_{12} \\ f_{13}\mathbf{Q}_{13} \\ f_{23}\mathbf{Q}_{23} \end{pmatrix}, \quad (28)$$

where

$$\begin{aligned}\mathbf{D} &= \begin{pmatrix} D_{h12} & D_{h13} & D_{h23} \\ D_{k12} & D_{k13} & D_{k23} \\ D_{l12} & D_{l13} & D_{l23} \end{pmatrix} \\ &= \begin{pmatrix} C_{hx}\sum_{12} + iS_{hx}\sum_2 & C_{hx}\sum_{13} + iS_{hx}\sum_3 & C_{hx}\sum_{23} + iS_{hx}\sum_{123} \\ C_{ky}\sum_{12} + iS_{ky}\sum_1 & C_{ky}\sum_{13} + iS_{ky}\sum_{123} & C_{ky}\sum_{23} + iS_{ky}\sum_3 \\ C_{lz}\sum_{12} + iS_{lz}\sum_{123} & C_{lz}\sum_{13} + iS_{lz}\sum_1 & C_{lz}\sum_{23} + iS_{lz}\sum_2 \end{pmatrix}. \end{aligned} \quad (29)$$

For the monoclinic and orthorhombic space groups, the transformation matrix $\mathbf{B}_0$ is

$$\mathbf{B}_0 = \begin{pmatrix} 1 & 0 & c \\ 0 & 1 & 0 \\ 0 & 0 & s \end{pmatrix}, \tag{30}$$

where $c = \cos\beta^*$, $s = \sin\beta^*$.

With reference to the scattering geometry of Fig. 1 and with the assumption that the crystal is mounted with $\mathbf{a}_0^* \| X_D$ and $\mathbf{b}_0^* \| Y_D$, the systems C and D coincide for $h00$ reflections ($\varphi = 0$, $\xi = 0$). For $0k0$ and $00l$ reflections, rotations ($\varphi = -90°$, $\xi = 0$) and ($\varphi = 0$, $\xi = \beta^*$), respectively, give the diffracting positions. Thus, for monoclinic crystals, $\mathbf{X}_0(\beta^*)$ and $\mathbf{B}_0(\beta^*)$ lead to a somewhat more complicated description.

In accordance with the recipe outlined in § 2.1, the matrix multiplications involving $\mathbf{\Phi}_0$, $\mathbf{X}_0$ and $\mathbf{B}_0$ have to be carried out on each of the elements of $\mathbf{D}$, leading to

$$\begin{pmatrix} \mathbf{F}(h00)_D \\ \mathbf{F}(0k0)_D \\ \mathbf{F}(00l)_D \end{pmatrix} = o/s\mathbf{D}_1 \begin{pmatrix} \mathbf{Q}_{xy} \\ \mathbf{Q}_{xz} \\ \mathbf{Q}_{yz} \\ \mathbf{Q}_{zz} \end{pmatrix}, \tag{31}$$

where

$$\mathbf{D}_1 = \begin{pmatrix} sD_{h12}f_{12} & D_{h13}f_{13} \\ -sD_{k12}f_{12} & D_{k23}f_{23} - cD_{k12}f_{12} \\ sD_{l23}f_{23} & -D_{l13}f_{13} \end{pmatrix}$$

$$\begin{pmatrix} D_{h23}f_{23} - cD_{h12}f_{12} & -2c/sD_{h13}f_{13} \\ -D_{k13}f_{13} & -2c/sD_{k13}f_{13} \\ cD_{l23}f_{23} - D_{l12}f_{12} & -2c/sD_{l13}f_{13} \end{pmatrix}. \tag{32}$$

In the next step, the complex values of the scattering contributions $\Phi_{\eta\nu}(\mathbf{h}, \Psi)$ are calculated according to (15) and (16),

$$\begin{pmatrix} \Phi_{\eta\nu}(h00, \Psi) \\ \Phi_{\eta\nu}(0k0, \Psi) \\ \Phi_{\eta\nu}(00l, \Psi) \end{pmatrix} = o/s\mathbf{D}_1 \begin{pmatrix} q_{xy}(\eta\nu, \Psi) \\ q_{xz}(\eta\nu, \Psi) \\ q_{yz}(\eta\nu, \Psi) \\ q_{zz}(\eta\nu, \Psi) \end{pmatrix}. \tag{33}$$

Explicit expressions for the PSFs of 'forbidden' axial reflections are given in the Appendix [(*A*1)-(*A*6)]. These equations apply to any appropriate monoclinic or orthorhombic space group. The total Ψ-dependent intensity follows then from

$$I(\mathbf{h}, \Psi) = (K_h/\sin 2\Theta)[|\Phi_{\sigma'\sigma}(\mathbf{h}, \Psi)|^2 + |\Phi_{\pi'\sigma}(\mathbf{h}, \Psi)|^2]. \tag{34}$$

$K_\mathbf{h}$ is a scale factor, $1/\sin 2\Theta$ is the Lorentz correction, absorption correction is neglected and the polarization correction is contained in the Φ elements.

3.1. *The* $\sum$ *sums*

With respect to partial-structure information contained in FRED, only centric projections are useful. Acentric projections occur in space groups in which the origin is arbitrary on the projection axis. (In other words, partial-structure information cannot be obtained where it is unnecessary.) Nevertheless, such a case does not preclude the existence of FRED, but the intensity must not depend on the edge atom's position. This may be verified considering $\Phi_{\sigma'\sigma}(h00, \Psi)$ and $\Phi_{\pi'\sigma}(h00, \Psi)$ given in the Appendix. For an acentric projection onto [100], all $R_{11,p} = 1$ so that

$$\sum_{123} = \sum_{23}, \quad \sum_2 = \sum_{12} \quad \text{and} \quad \sum_3 = \sum_{13}. \tag{35}$$

Consequently, both PSFs can be factorized with respect to $[C_{hx} + iS_{hx}]$, which disappears upon calculating $|\Phi_{\sigma'\sigma}(h00, \Psi)|^2$ and $|\Phi_{\pi'\sigma}(h00, \Psi)|^2$.

For the centric projections of structures (with or without an inversion centre), the properties of $\Phi_{\sigma'\sigma}$ and $\Phi_{\pi'\sigma}$ depend on the total space-group symmetry. If there is an inversion centre, it is obvious that

$$\sum_{123} = \sum_{p=1}^{m} s_p \det(\mathbf{R}_p) = 0 \tag{36}$$

since $\det(\mathbf{R}_p)$ changes sign for the inverse operations while s_p does not. The same argument holds for the sums involving only one R_{ii} element, *i.e.* $\sum_1 = \sum_2 = \sum_3 = 0$.

Thus, for centric space groups, only sums $\sum_{ij}$ are significant and $\Phi_{\sigma'\sigma}$ and $\Phi_{\pi'\sigma}$ simplify as expected by omission of the imaginary part of the geometric term of the 'edge atom'. Still in agreement with the conventional scattering model, the PSFs are complex quantities in the case of AAS.

For the 'forbidden' axial reflections, there are always $m/2$ s_p terms of either sign. Additionally, $R_{ii,p}$, $R_{ii,p} \times R_{jj,p}$ and $\det(\mathbf{R}_p)$ are also either all positive or pairwise positive and negative. Combining these possibilities shows that the $\sum$ sums must be equal to 0 or m. Thus, dividing the $\sum$ sums by the number of symmetry operations m in the space group, yields $\sum = 0$ or 1. Therefore, (*A*1)-(*A*6) are m-multiples of PSFs describing the scattering per asymmetric unit.

3.2. *Systematic representation*

According to (27), Table 2 gives a complete representation of the 45 monoclinic and orthorhombic space groups allowing for FRED of *axial* reflections. This compilation is based on *International Tables for Crystallography* (1983). For the monoclinic system, only the standard second setting is considered.

The space groups are indexed by their numbers. Within each point-group box the space groups are classified according to a 'reduced symmetry' (RS), *i.e.* a unique combination of *relevant* symmetry elements that must be contained in the full symmetry to

Table 2. *Forbidden reflections in point groups* 2, 2/*m*, 222, *mm*2 *and mmm*

a', *b'* and *c'* denote glide planes with translations $a_0/4$, $b_0/4$ and $c_0/4$, respectively. + indicates a nonvanishing sum. $D_{\tau ij}$ are elements of (29), where $\tau = h$, k or l. For other details see text.

Point group	Reduced symmetry	Space-group no.	*h k l*	$\sum_1$	$\sum_2$	$\sum_3$	$\sum_{12}$	$\sum_{13}$	$\sum_{23}$	$\sum_{123}$	$D_{\tau 12}$	$D_{\tau 13}$	$D_{\tau 23}$
2	$*2_1*$	(4)	0 *k* 0	+		+	+		+		$C_{ky} + iS_{ky}$		$C_{ky} + iS_{ky}$
m	**c**	(7, 9)	0 0 *l*		+		+		+	+	$C_{lz} + iS_{lz}$		$C_{lz} + iS_{lz}$
2/*m*	$*2_1*$	(11, 14)	0 *k* 0				+		+		C_{ky}		C_{ky}
	c	(13, 14, 15)	0 0 *l*				+		+		C_{lz}		C_{lz}
222	$2_12_12_1$	(19)	*h* 0 0		+			+			iS_{hx}	C_{hx}	
	2_12_1*	(18)				+	+				C_{hx}	iS_{hx}	
		(18, 19)	0 *k* 0			+	+				C_{ky}		iS_{ky}
	$**2_1$	(17, 19, 20)	0 0 *l*	+					+			iS_{lz}	C_{lz}
*mm*2	$*a2_1$	(31)	*h* 0 0		+				+		iS_{hx}		C_{hx}
	a	(28, 29, 32, 33, 34, 40, 41)					+			+	C_{hx}		iS_{hx}
	a'	(43)											
	*b***	(30, 32, 33, 34)	0 *k* 0				+			+	C_{ky}	iS_{ky}	
	*b'***	(43)											
	$c*2_1$	(29, 33)	0 0 *l*	+				+				$C_{lz} + iS_{lz}$	
	$*c2_1$	(26, 31, 36)			+				+				$C_{lz} + iS_{lz}$
	*cc**	(27, 30, 34, 37)					+			+	$C_{lz} + iS_{lz}$		
	*c'c'**	(43)											
mmm	2_1a*	(55, 58)	*h* 0 0				+				C_{hx}		
	2_1*a	(51, 54, 56, 59, 60, 61, 62)						+				C_{hx}	
	**aa*	(48, 50, 52, 53)							+				C_{hx}
	**a'a'*	(70)											
	$b2_1*$	(52, 5, 57, 58, 61, 62)	0 *k* 0				+				C_{ky}		
	$*2_1b$	(56, 59)							+				C_{ky}
	*b*b*	(48, 50, 60)						+				C_{ky}	
	*b'*b'*	(70)											
	$c*2_1$	(62)	0 0 *l*					+				C_{lz}	
	$*c2_1$	(53, 57, 60, 61, 63, 64)							+				C_{lz}
	*cc**	(48, 49, 52, 54, 56, 58, 66, 68)					+				C_{lz}		
	*c'c'**	(70)											

yield identical combinations of $\sum$ sums and hence identical PSFs, $\Phi_{\sigma'\sigma}$ and $\Phi_{\pi'\sigma}$. These symmetry elements are either one or two glide planes parallel to **h** possessing a glide component along **h** and/or the 2_1 axes. An asterisk indicates a 'wild card', *i.e.* the symmetry element(s) associated with the corresponding direction is (are) irrelevant.

For the 6 point groups and the 3 types of axial reflections, one finds 23 different cases to be considered in the investigation of $I(\mathbf{h}, \Psi)$. Only 18 of them can yield partial-structure information due to a fixed origin with respect to the considered crystal axis.

For each space group, the entries of the $\sum$ sums are all either blank or +, indicating $\sum = 0$ or $\sum = m$, respectively. Thus, for any monoclinic or orthorhombic space group, Table 2 shows whether or not FRED can occur and, if so, which $\sum$ sums ($= m$) have to be considered in the calculations of $\Phi_{\sigma'\sigma}(\mathbf{h}, \Psi)$ and $\Phi_{\pi'\sigma}(\mathbf{h}, \Psi)$. Table 2 confirms that the centric space groups exhibit only one (orthorhombic) or two (monoclinic) $\sum_{ij}$ contribution(s), while all acentric space groups are associated with mixed $\sum$ types, as already stated in deriving (36).

Table 3 summarizes the 23 RS cases (column 2) distributed over the point groups (column 1). Column 3 contains the numbers of the space groups belonging to each case and column 4 contains the reflection type considered. The last two columns give explicit expressions for $|\Phi_{\sigma'\sigma}(\mathbf{h}, \Psi)|^2$ and $|\Phi_{\pi'\sigma}(\mathbf{h}, \Psi)|^2$, multiplied by the factor $s^4/(om)^2$. Column 5 numbers the cases [1, ..., 23] mentioned above. Thus, Table 3 provides the basis for a systematic inspection of axial FRED in monoclinic and orthorhombic systems, in particular with respect to the 18 distinguishable cases where partial-structure information is contained in the 'forbidden' reflections. In agreement with Table 2, these are the RS cases for which the geometric terms $C_{\mathbf{h}\cdot\mathbf{r}}$ and/or $S_{\mathbf{h}\cdot\mathbf{r}}$ appear in Table 3, indicating a centre of inversion for the projected structure.

3.3. *Examples*

The use of Table 3 may be illustrated by two examples.

(1) *Point group mm*2, '*reduced symmetry*' **a**, *reflections h*00. From Table 2, all $\sum$ vanish except $\sum_{12} = \sum_{123} = m$. Then, using [10] of Table 3,

$$|\Phi_{\sigma'\sigma}(h00, \Psi)|^2 = (om)^2 s^{-4} S_{hx}^2 |f_{23}|^2 S_{2\Psi}^2,$$

$$|\Phi_{\pi'\sigma}(h00, \Psi)|^2 = (om)^2 s^{-4} |C_{hx} f_{12} C_\Theta S_\Psi + iS_{hx} f_{23} S_\Theta C_{2\Psi}|^2.$$

These results are valid for the space groups *Pma*2 (No. 28), *Pca*2_1 (No. 29), *Pba*2 (No. 32), *Aba*2 (No. 41), *Pna*2_1 (No. 33), *Ama*2 (No. 40) and *Pnn*2 (No. 34), for the last one because the *n*-glide plane perpendicular to [010] contains an *a*-glide component.

(2) *Point group mmm* '*reduced symmetry*' $*2_1b$, *reflections* $0k0$. From Table 2, all $\sum$ vanish except

Table 3. *'Polarized structure factors' for the* 23 *'reduced symmetry' cases up to orthorhombic symmetry*

Point group	Reduced symmetry	Space-group no.	h k l	Number	$s^4(om)^{-2}\|\Phi_{\sigma'\sigma}(\mathbf{h}, \Psi)\|^2$	$s^4(om)^{-2}\|\Phi_{\pi'\sigma}(\mathbf{h}, \Psi)\|^2$
2	$*2_1*$	(4)	0 k 0	[1]		$\|f_{12}(sS_\Psi - cC_\Psi) + f_{23}C_\Psi\|^2 s^2 C^2_\Theta$
m	$*c*$	(7, 9)	0 0 l	[2]	$\|f_{12} - cf_{23}\|^2 s^2 S^2_{2\Psi}$	$\|f_{12}S_\Theta C_{2\Psi} - f_{23}(sC_\Theta S_\Psi + cS_\Theta C_{2\Psi})\|^2 s^2$
$2/m$	$*2_1*$	(11, 14)	0 k 0	[3]		$C^2_{k\lambda}*[1]$
	$*c*$	(13, 14, 15)	0 0 l	[4]	$C^2_{lz}*[2]$	$C^2_{lz}*[2]$
222	$2_12_12_1$	(19)	h 0 0	[5]		$\|C_{h\lambda}f_{13}C_\Psi - iS_{h\lambda}f_{12}S_\Psi\|^2 C^2_\Theta$
	2_12_1*	(18)		[6]		$\|C_{h\lambda}f_{12}S_\Psi - iS_{h\lambda}f_{13}C_\Psi\|^2 C^2_\Theta$
		(18, 19)	0 k 0	[7]		$\|C_{k\lambda}f_{12}S_\Psi + iS_{k\lambda}f_{23}C_\Psi\|^2 C^2_\Theta$
	$**2_1$	(17, 19, 20)	0 0 l	[8]		$\|C_{lz}f_{23}S_\Psi + iS_{lz}f_{13}C_\Psi\|^2 C^2_\Theta$
$mm2$	$*a2_1$	(31)	h 0 0	[9]	$C^2_{h\lambda}\|f_{23}\|^2 S^2_{2\Psi}$	$\|C_{h\lambda}f_{23}S_\Theta C_{2\Psi} + iS_{h\lambda}f_{12}C_\Theta S_\Psi\|^2$
	$*a*$	(28, 29, 32, 33, 34, 40, 41)		[10]	$S^2_{h\lambda}\|f_{23}\|^2 S^2_{2\Psi}$	$\|C_{h\lambda}f_{12}C_\Theta S_\Psi + iS_{h\lambda}f_{23}S_\Theta C_{2\Psi}\|^2$
	$*a'*$	(43)				
	$b**$	(30, 32, 33, 34)	0 k 0	[11]	$S^2_{k\lambda}\|f_{13}\|^2 S^2_{2\Psi}$	$\|C_{k\lambda}f_{12}C_\Theta S_\Psi + iS_{k\lambda}f_{13}S_\Theta C_{2\Psi}\|^2$
	$b'**$	(43)				
	$c*2_1$	(29, 33)	0 0 l	[12]		$\|f_{13}\|^2 C^2_\Theta C^2_\Psi$
	$*c2_1$	(26, 31, 36)		[13]		$\|f_{23}\|^2 C^2_\Theta S^2_\Psi$
	$cc*$	(27, 30, 34, 37)		[14]	$\|f_{12}\|^2 C^2_{2\Psi}$	$\|f_{12}\|^2 S^2_\Theta C^2_{2\Psi}$
	$c'c'*$	(43)				
mmm	2_1a*	(55, 58)	h 0 0	[15]		$C^2_{h\lambda}\|f_{12}\|^2 C^2_\Theta S^2_\Psi$
	2_1*a	(51, 54, 56, 59, 60, 61, 62)		[16]		$C^2_{h\lambda}*[12]$
	$*aa$	(48, 50, 52, 53)		[17]	$C^2_{h\lambda}\|f_{23}\|^2 S^2_{2\Psi}$	$C^2_{h\lambda}\|f_{23}\|^2 S^2_\Theta C^2_{2\Psi}$
	$*a'a'$	(70)				
	$b2_1*$	(52, 55, 57, 58, 61, 62)	0 k 0	[18]		$C^2_{k\lambda}\|f_{12}\|^2 C^2_\Theta S^2_\Psi$
	$*2_1b$	(56, 59)		[19]		$C^2_{k\lambda}\|f_{23}\|^2 C^2_\Theta C^2_\Psi$
	$b*b$	(48, 50, 60)		[20]	$C^2_{k\lambda}\|f_{13}\|^2 S^2_{2\Psi}$	$C^2_{k\lambda}\|f_{13}\|^2 S^2_\Theta C^2_{2\Psi}$
	$b'*b'$	(70)				
	$c*2_1$	(62)	0 0 l	[21]		$C^2_{lz}*[12]$
	$*c2_1$	(53, 57, 60, 61, 63, 64)		[22]		$C^2_{lz}*[13]$
	$cc*$	(48, 49, 52, 54, 56, 58, 66, 68)		[23]	$C^2_{lz}*[14]$	$C^2_{lz}*[14]$
	$c'c'*$	(70)				

$\sum_{23} = m$. Then, from Table 3 [19],

$$\Phi_{\sigma'\sigma}(0k0, \Psi) = 0,$$

i.e. the scattered radiation is π polarized,

$$|\Phi_{\pi'\sigma}(0k0, \Psi)|^2 = (om)^2 s^{-4} C^2_{k\lambda}|f_{23}|^2 C^2_\Theta C^2_\Psi$$

for the space groups $P2_1/c2_1/c2/n$ (No. 56) and $P2_1/m2_1/m2/n$ (No. 59). In both cases the relevant symmetry elements are the 2_1 axis parallel to [010] and the n-glide plane perpendicular to [001], containing a $b/2$ translation.

3.4. *Symmetry elements and scattering contributions – principles in 'polarized structure factors'*

A closer inspection of Table 3 in terms of the $\sigma'\sigma$ and $\pi'\sigma$ contributions to the total scattering reveals the following correlations.

(i) A 2_1 axis in the direction of the (axial) scattering vector **h** prohibits a $|\Phi_{\sigma'\sigma}|^2$ term. This can be easily understood by considering that for an odd index, *e.g.* h, $\Phi_{\sigma'\sigma}$ involves only the difference of the 2_1-related scattering-factor tensors, $\mathbf{f}_D$, projected onto $[001]_D$. These projections are equal, thus $\Phi_{\sigma'\sigma}$ must vanish *via* the geometric terms. Consequently, a 2_1 axis along **h** always produces scattered radiation whose polarization is π if that of the incoming radiation is σ (and *vice versa*).

(ii) If there is a nonvanishing contribution $|\Phi_{\sigma'\sigma}|^2$, it is due to a single or to two mutually orthogonal glide planes parallel to **h** possessing translation components along **h**. $|\Phi_{\sigma'\sigma}|^2$ is independent of Θ and it must be periodic in $\pi/2$ according to its $S_{2\Psi}$ dependence (see Table 1).

(iii) For an atom in a general position, there is always a $|\Phi_{\pi'\sigma}|^2$ contribution to the scattering. If a 2_1 axis is parallel to **h**, this component is periodic in π and strictly proportional to C^2_Θ for all relevant orthorhombic space groups, whereas the two monoclinic cases [1] and [3], *i.e.* RS = $*2_1*$, allow more complicated patterns.

(iv) If there is no 2_1 axis parallel to **h** in an orthorhombic space group, $\Phi_{\pi'\sigma}$ is periodic in either $\pi/2$ (point groups $mm2$ and mmm) or 2π, the latter indicating a space group belonging to one of the cases [9], [10], [11] of point $mm2$. Additionally, $I(\mathbf{h}, \Psi)$ contains a Θ-independent contribution [see (ii)].

Further rules may be extracted, for instance with respect to atoms located at special positions, *e.g.* with x, y, $z = 0$, $\frac{1}{4}$ or $\frac{1}{8}$. Here it suffices to emphasize that the investigation of both the polarization of the scattered radiation and the Ψ pattern of the intensity may be useful for obtaining symmetry information in difficult cases (*e.g.* pseudosymmetric structures, phase transitions).

4. FRED and partial-structure information

In this section, the 18 relevant cases of Table 3 are discussed in terms of assessing the 'edge atom's' coordinate corresponding to the considered direction **h**. According to Table 3, 'edge-atom' information cannot be obtained in the point groups 2 and m

Table 4. Ψ_1, Ψ_2 *settings of crystal yielding* R_{ij}^C *and* R_{ij}^S, *respectively*

Point group	Reduced symmetry	h k l	Ψ_1	p	Ψ_2	p
$2/m$	$*2_1*$	0 k 0	$0, \pm\pi/2, \pi$	1		
	$*c*$	0 0 l	$0, \pi$	−1		
222	2_12_1*	h 0 0	$\pm\pi/2$	1	$0, \pi$	1
		0 k 0	$\pm\pi/2$	1	$0, \pi$	1
	$**2_1$	0 0 l	$\pm\pi/2$	1	$0, \pi$	1
	$2_12_12_1$	h 0 0	$0, \pi$	1	$\pm\pi/2$	1
$mm2$	$*a2_1$	h 0 0	$0, \pi$	−1		
	$*a*$ or $*a'*$				$0, \pi$	−1
	$b**$ or $b'**$	0 k 0			$0, \pi$	−1
mmm	2_1a*	h 0 0	$\pm\pi/2$	1		
	2_1*a		$0, \pi$	1		
	$*aa$ or $*a'a'$		$0, \pm\pi/2, \pi, \pm\pi/4, \pm3\pi/4$	−1		
	$b2_1*$	0 k 0	$\pm\pi/2$	1		
	$*2_1b$		$0, \pi$	1		
	$b*b$ or $b'*b'$		$0, \pm\pi/2, \pi, \pm\pi/4, \pm3\pi/4$	−1		
	$c*2_1$	0 0 l	$0, \pi$	1		
	$*c2_1$		$\pm\pi/2$	1		
	$cc*$ or $c'c'*$		$0, \pm\pi/2, \pi, \pm\pi/4, \pm3\pi/4$	−1		

because the Ψ-dependent PSFs $|\Phi_{\sigma'\sigma}(\mathbf{h}, \Psi)|^2$ and $|\Phi_{\pi'\sigma}(\mathbf{h}, \Psi)|^2$ do not contain terms C_{hx}, S_{hx} *etc.* For monoclinic systems there is 'edge-atom' information only in point group $2/m$.

The method of KP*a* uses the comparison of the intensities of any two 'forbidden' axial reflections of the same kind. The intensity values are taken at settings Ψ_i, suitable to eliminate in the intensity ratio the *a priori* unknown off-diagonal element(s) of the scattering-factor tensor (*i.e.* the anisotropy of the resonance). Thus, provided there are significant FRED signals, neither the physical origin of the anisotropy nor its absolute magnitude need to be known.

By analysing the intensity ratio, one can obtain for all cases

$$R_{ij}^C = \cos^2(2\pi\mathbf{h}_i\cdot\mathbf{r})/\cos^2(2\pi\mathbf{h}_j\cdot\mathbf{r}) = (K_{\mathbf{h}_j}/K_{\mathbf{h}_i})T_{ij}^p[I(\mathbf{h}_i, \Psi_1)/I(\mathbf{h}_j, \Psi_1)] \quad (37)$$

and/or

$$R_{ij}^S = \sin^2(2\pi\mathbf{h}_i\cdot\mathbf{r})/\sin^2(2\pi\mathbf{h}_j\cdot\mathbf{r}) = (K_{\mathbf{h}_j}/K_{\mathbf{h}_i})T_{ij}^p[I(\mathbf{h}_i, \Psi_2)/I(\mathbf{h}_j, \Psi_2)], \quad (38)$$

where $T_{ij} = \tan\Theta_i/\tan\Theta_j$ is a geometric factor and incorporates the Lorentz correction. $K_{\mathbf{h}_i}$ and $K_{\mathbf{h}_j}$ are scale factors for the two reflections. The exponent p is +1 if the 'reduced symmetry' indicates a 2_1 axis parallel to $\mathbf{h}$; otherwise, $p = -1$.

Table 4 gives values of p, Ψ_1 and Ψ_2 (appearing in the expressions for R_{ij}^C and R_{ij}^S). It provides supplementary information to Table 3 and shows how to determine R_{ij}^C and/or R_{ij}^S for a given space group of interest. Under the provision that the (potentially $\mathbf{h}$-dependent) scale factors $K_{\mathbf{h}}$ are known or that the reflection intensities can be put on a common scale, *i.e.* $K_{\mathbf{h}_j}/K_{\mathbf{h}_i} = 1$, the T_{ij}^p-corrected intensity ratios R_{ij}^C, R_{ij}^S give indications about allowed ranges of fractional-coordinate values. This information is still ambiguous, but it can be improved to become a unique indication of the symmetry-equivalent coordinates by combining increasing numbers of reflections into corresponding R_{ij}^C and/or R_{ij}^S quantities.

In contrast to centric space groups, acentric space groups possess freedom from scaling. In point group 222, the quantities R_{ij}^C and R_{ij}^S can be obtained simultaneously in the same diffracting position but for different Ψ settings. Thus, it is possible to eliminate the scaling by calculating

$$R_{ij}^T = R_{ij}^S/R_{ij}^C = \tan^2(2\pi\mathbf{h}_i\cdot\mathbf{r})/\tan^2(2\pi\mathbf{h}_j\cdot\mathbf{r}) = [I(\mathbf{h}_i, \Psi_2)/I(\mathbf{h}_j, \Psi_2)]*[I(\mathbf{h}_j, \Psi_1)/I(\mathbf{h}_i, \Psi_1)]. \quad (39)$$

For space group $P2_12_12_1$, this has been discussed in detail by Kirfel & Petcov (KP*a*), and experimental evidence of the approach was given in a test on a crystal of $LiHSeO_3$ (KP*b*). In the latter paper, it was also shown that the coexisting anisotropy of absorption may have to be taken into account, which, however, is neglected in the present context.

The remaining cases in point group $mm2$ present a somewhat more complicated situation. There is, however, also a combination of Ψ settings that offers the possibility of eliminating the scale factors $K_{\mathbf{h}}$. Using $\Psi_1 = \Psi_1$ or Ψ_2 of Table 4 and $\Psi_2 = \pm\pi/4$, $\pm3\pi/4$, one obtains again a quantity R_{ij}^T that is independent of scaling,

$$R_{ij}^T = \frac{\tan^2(2\pi\mathbf{h}_i\cdot\mathbf{r})}{\tan^2(2\pi\mathbf{h}_j\cdot\mathbf{r})} = \frac{[I(\mathbf{h}_j, \Psi_2)\sin^2\Theta_j - I(\mathbf{h}_j, \Psi_1)]}{[I(\mathbf{h}_i, \Psi_2)\sin^2\Theta_i - I(\mathbf{h}_i, \Psi_1)]}\,\frac{I(\mathbf{h}_i, \Psi_1)\cos^2\Theta_i}{I(\mathbf{h}_j, \Psi_1)\cos^2\Theta_j} \quad (40)$$

for cases [10], $*a*$ and [11], $b**$; one obtains the inverse, $1/R_{ij}^T$, for [9], $*a2_1$.

Thus, it should be possible to obtain partial-structure information in all possible cases by relating selected intensity values of different axial reflections of the same type. The appropriate Ψ settings are given in Table 4. For all centric space groups, the intensities must be scaled together, for the acentric ones, scaling is unnecessary according to (39) and (40).

5. Summary

The general treatment of kinematic X-ray diffraction of totally polarized radiation in the presence of AAS allows a clear distinction of geometric and structural (physical) aspects. This distinction follows from expanding the structure-factor tensor $\mathbf{F}(\mathbf{h})_D$, defined in the diffractometer system, into a complex linear

combination of six real basic tensors $\mathbf{Q}'_{uv}$ ($u, v = x, y, z$) that are fixed with respect to the crystal. The index surfaces of the $\mathbf{Q}'_{uv}$ are surface spherical harmonics, *i.e.* p_u^2 and d_{uv} functions. Thus, the Ψ-dependent scattering of the σ- and π-polarized components of the incident radiation can be treated as scattering from those basic scatterers, each giving well defined dependencies of the scattering contributions from the azimuthal setting (Ψ) of the crystal and also from the scattering angle (2Θ) if polarization parallel to the scattering plane is involved. Calculating the real quantities $q_{uv}(\eta\nu, \Psi) = \mathbf{e}_\eta^T \mathbf{Q}'_{uv}(\Psi)\mathbf{e}_\nu$, where $\mathbf{e}_\eta$, $\mathbf{e}_\nu$ ($\eta = \sigma', \pi'$ and $\nu = \sigma, \pi$) are unit vectors of polarization directions, one obtains a basis set of real functions that fully describe the geometrical aspect of the scattering. Since $\sum_{u=1,u\le v}^{3} q_{uv}$ reduce to 0, 1 and $\cos 2\Theta$ if $\mathbf{F}(\mathbf{h})_D \propto \mathbf{I}$ (*i.e.* the isotropic case), it is evident that separating the geometric aspect is equivalent to describing an extension of the polarization correction of the Thomson scattering model. For $\eta = \nu = \sigma$, the q_{uv} are recognized as the Ψ-dependent projections of the tensors $\mathbf{Q}'_{uv}$ onto $\mathbf{e}_\sigma$, implying that these functions simply probe the respective index surfaces perpendicular to the scattering vector **h**. For the other cases, $\eta \neq \nu$, each $q_{uv}(\eta\nu, \Psi)$ is the gradient vector of the corresponding characteristic tensor surface, taken at $\mathbf{e}_\nu$ and projected onto $\mathbf{e}_\eta$. The geometrical basis functions are valid for all crystals and the angular dependencies of reflection intensities [in particular the periodicities of the $I(\mathbf{h}, \Psi)$ patterns] are therefore exclusively determined by the scattering geometry.

The nature of the crystal, *i.e.* the space group and physical content of the asymmetric unit, determines the second aspect, which is contained in the complex coefficients combining the q_{uv} to linear combinations $\Phi_{\eta\nu}(\mathbf{h}, \Psi)$. These complex quantities may be termed 'polarized structure factors'. Thus, any modelling of the scattering consists essentially in calculating the coefficients according to the structural information available. Since they incorporate the energy-dependent atomic-scattering-factor contributions due to AAS, a polarized structure factor $\Phi_{\eta\nu}(\mathbf{h}, \Psi)$ is only constant for fixed energy. Once the coefficients are formulated, the total scattered radiation follows from the linear combination of the PSF weighted with the amplitudes of the σ and π components of the incident plane wave and the total (polarization-corrected) scattered intensity is the complex-conjugated product.

Scattering in the presence of AAS can thus be evaluated in a step-by-step procedure that involves, as the central task, the development of the structure-dependent coefficients. With this point of view, programming can be carried out with clear guidelines.

Following the developed treatment, a systematic investigation of 'forbidden' axial reflections in monoclinic and orthorhombic space groups was carried out. If the problem is confined to purely σ-polarized primary radiation and one 'edge atom' per asymmetric unit, the formulation of the coefficients is straightforward by virtue of having only diagonal elements in the rotation matrices of the symmetry operations. The compilation of the results shows that the 45 space groups permitting FRED can be classified into 23 'reduced symmetry' cases according to point-group symmetry and characteristic combinations of symmetry elements with translation components along **h**. When the axial extinction rules are violated, the polarization properties of the scattered radiation are characteristic with respect to the presence or absence of a 2_1 axis parallel to **h** so that combined intensity and polarization measurements could be employed in difficult symmetry cases, *e.g.* pseudosymmetry, phase transitions. In addition to the concise report of axial FRED presenting a useful survey for both planning an experiment and evaluating results, it is shown in particular how partial-structure information, *i.e.* possible locations of the 'edge atom', may be obtained from only a few 'forbidden' axial reflections measured at appropriate Ψ settings of the crystal. Attractively, the method depends only on the presence of AAS, but no further knowledge about its origin or magnitude is required. In acentric structures, even common scaling of the intensity patterns is unnecessary. Owing to the great experimental effort and costs required, the method may not be routinely applied. Therefore, it will by no means become competitive to any established structure-solution method, but it is conceivable that occasionally it may help to 'get a foot in the door' for difficult phasing problems.

This study has received financial support from the Deutsche Forschungsgemeinschaft, which is gratefully acknowledged. Our special thanks are due to Professor Dr K. Fischer, Universität des Saarlandes, Germany, for many fruitful discussions.

APPENDIX

Explicit 'polarized structure factors', PSF, for 'forbidden' axial reflections

*h*00 *reflections* (*h odd*)

$$\begin{aligned}\Phi_{\sigma'\sigma}(h00, \Psi) &= (o/s^2)\{C_{hx}[f_{12}\textstyle\sum_{12} scS_{2\Psi} - 2f_{13}\sum_{13} cC_\Psi^2 \\ &\quad - f_{23}\textstyle\sum_{23} sS_{2\Psi}] \\ &\quad + iS_{hx}[f_{12}\textstyle\sum_{2} scS_{2\Psi} - 2f_{13}\sum_{3} cC_\Psi^2 \\ &\quad - f_{23}\textstyle\sum_{123} sS_{2\Psi}]\}, \end{aligned} \tag{A1}$$

$$\Phi_{\pi'\sigma}(h00, \Psi)$$
$$= (o/s^2)\{C_{hx}[f_{12}\textstyle\sum_{12}(scS_\Theta C_{2\Psi} - s^2 C_\Theta S_\Psi)$$
$$+ f_{13}\textstyle\sum_{13}(sC_\Theta C_\Psi + cS_\Theta S_{2\Psi}) - f_{23}\textstyle\sum_{23} sS_\Theta C_{2\Psi}]$$
$$+ iS_{hx}[f_{12}\textstyle\sum_{2}(scS_\Theta C_{2\Psi} - s^2 C_\Theta S_\Psi)$$
$$+ f_{13}\textstyle\sum_{3}(sC_\Theta C_\Psi + cS_\Theta S_{2\Psi})$$
$$- f_{23}\textstyle\sum_{123} sS_\Theta C_{2\Psi}]\}. \qquad (A2)$$

0k0 reflections (k odd)

$$\Phi_{\sigma'\sigma}(0k0, \Psi)$$
$$= (o/s^2)\{C_{ky} f_{13}\textstyle\sum_{13}(sS_{2\Psi} - 2cC_\Psi^2)$$
$$+ iS_{ky} f_{13}\textstyle\sum_{123}(sS_{2\Psi} - 2cC_\Psi^2)\}, \qquad (A3)$$

$$\Phi_{\pi'\sigma}(0k0, \Psi)$$
$$= (o/s^2)\{C_{ky}[f_{12}\textstyle\sum_{12} C_\Theta(s^2 S_\Psi - scC_\Psi)$$
$$+ f_{13}\textstyle\sum_{13} S_\Theta(sC_{2\Psi} + cS_{2\Psi}) + f_{23}\textstyle\sum_{23} sC_\Theta C_\Psi]$$
$$+ iS_{ky}[f_{12}\textstyle\sum_{1} C_\Theta(s^2 S_\Psi - scC_\Psi)$$
$$+ f_{13}\textstyle\sum_{123} S_\Theta(sC_{2\Psi} + cS_{2\Psi})$$
$$+ f_{23}\textstyle\sum_{3} sC_\Theta C_\Psi]\}. \qquad (A4)$$

00l reflections (l odd)

$$\Phi_{\sigma'\sigma}(00l, \Psi)$$
$$= (o/s^2)\{C_{lz}[f_{12}\textstyle\sum_{12} sS_{2\Psi} - 2f_{13}\textstyle\sum_{13} cC_\Psi^2$$
$$- f_{23}\textstyle\sum_{23} scS_{2\Psi}]$$
$$+ iS_{lz}[f_{12}\textstyle\sum_{123} sS_{2\Psi} - 2f_{13}\textstyle\sum_{1} cC_\Psi^2$$
$$- f_{23}\textstyle\sum_{2} scS_{2\Psi}]\}, \qquad (A5)$$

$$\Phi_{\pi'\sigma}(00l, \Psi)$$
$$= (o/s^2)\{C_{lz}[f_{12}\textstyle\sum_{12} sS_\Theta C_{2\Psi}$$
$$+ f_{13}\textstyle\sum_{13}(-sC_\Theta C_\Psi + cS_\Theta S_{2\Psi})$$
$$- f_{23}\textstyle\sum_{23}(s^2 C_\Theta S_\Psi + scS_\Theta C_{2\Psi})]$$
$$+ iS_{lz}[f_{12}\textstyle\sum_{123} sS_\Theta C_{2\Psi}$$
$$+ f_{13}\textstyle\sum_{1}(-sC_\Theta C_\Psi + cS_\Theta S_{2\Psi})$$
$$- f_{23}\textstyle\sum_{2}(s^2 C_\Theta S_\Psi + scS_\Theta C_{2\Psi})]\}. \qquad (A6)$$

References

BUSING, W. R. & LEVY, H. A. (1967). *Acta Cryst.* **22**, 457-464.
DMITRIENKO, V. E. (1983). *Acta Cryst.* A**39**, 29-35.
DMITRIENKO, V. E. (1984). *Acta Cryst.* A**40**, 89-95.
FANCHON, E. & HENDRICKSON, W. A. (1990). *Acta Cryst.* A**46**, 809-820.
International Tables for Crystallography (1983). Vol. A. Dordrecht: Kluwer Academic Publishers.
KIRFEL, A. & PETCOV, A. (1991). *Z. Kristallogr.* **195**, 1-15.
KIRFEL, A. & PETCOV, A. (1992). *Acta Cryst.* A**48**, 247-259.
KIRFEL, A., PETCOV, A. & EICHHORN, K. (1991). *Acta Cryst.* A**47**, 180-195.
TEMPLETON, D. H. & TEMPLETON, L. K. (1980). *Acta Cryst.* A**36**, 237-241.
TEMPLETON, D. H. & TEMPLETON, L. K. (1982). *Acta Cryst.* A**38**, 62-67.
TEMPLETON, D. H. & TEMPLETON, L. K. (1985). *Acta Cryst.* A**41**, 133-142, 365-371.
TEMPLETON, D. H. & TEMPLETON, L. K. (1986). *Acta Cryst.* A**42**, 478-481.
TEMPLETON, L. K. & TEMPLETON, D. H. (1988). *Acta Cryst.* A**44**, 1045-1051.
WILLIS, B. T. M. & PRYOR, A. W. (1975). *Thermal vibrations in Crystallography*. Cambridge Univ. Press.

Acta Cryst. (1993). A**49**, 45-55

Methods Used in the Structure Determination of Foot-and-Mouth Disease Virus

BY ELIZABETH FRY, RAVINDRA ACHARYA* AND DAVID STUART

Laboratory of Molecular Biophysics, Rex Richards Building, South Parks Road, Oxford OX1 3QU, England

(*Received* 14 *March* 1992; *accepted* 13 *July* 1992)

Abstract

The structure of foot-and-mouth disease virus (FMDV) strain O_1 BFS 1860 has been determined to 2.9 Å resolution using the molecular-replacement method [Acharya, Fry, Stuart, Fox, Rowlands & Brown (1989). *Nature (London)*, **337**, 709-716]. Crystals of the virus with average dimensions 0.12 × 0.06 × 0.12 mm belong to space group $I23$, $a = 345$ Å with 1/12 of the icosahedral particle per asymmetric unit giving fivefold noncrystallographic redundancy. Oscillation diffraction photographs were collected at the SERC Synchrotron Radiation Source at Daresbury in accordance with strict disease security regulations. The ambiguity in particle orientation was resolved using a self-rotation function and starting estimates of the phases to 8 Å were derived from the known structures of two picornaviruses similarly oriented in the $I23$ unit cell. The phases were refined

* Present address: Department of Biochemistry, 4-West, University of Bath, Claverton Down, Bath BA2 7AY, England.

0108-7673/93/010045-11$06.00